JOURNAL OF MATERIALS SCIENCE 26 (1991) 4795–4802

Microstructure evolution during mechanical working of three RS aluminium alloys: Al–4Cr–1Fe, Al–5Cr–2Zr and Al–6.43Cr–1.67Zr

E. K. IOANNIDIS, T. SHEPPARD
Department of Materials, Imperial College of Science, Technology and Medicine, Exhibition Road, London SW7 2BP, UK

Three Al–Cr alloys containing additions of Zr and Fe have been fabricated via cold compaction and hot extrusion. The decomposition of the powder microstructure and the subsequent coarsening during thermomechanical treatment have been studied. Detailed electron microscopy investigations were performed at different locations of partially extruded billets at 450 °C. The microstructure of the dead metal zone reflects the effect the induction heating exerts on the as-atomized powder microstructure. In the low Cr alloys, Al–4Cr–1Fe and Al–5Cr–2Zr, decomposition of the rapidly solidified microstructure commences at the rich intercellular network, whereas the microstructure of the Al–6.43Cr–1.67Zr alloy remains relatively unaffected. Within the deformation zone the precipitation kinetics are affected by the shearing and the temperature rise. The cells and the powder particles are aligned along the extrusion direction. Precipitation is taking place within the primary segregation-free areas, observed in Al–4Cr–1Fe and Al–5Cr–2Zr alloys, whereas in the Al–6.43Cr–1.67Zr alloy, decomposition of the powder microstructure starts at the Cr-rich intermetallic particles. The as-extruded microstructure is fibrous and heterogeneous. The heterogeneity of the as-extruded microstructure is a result of the microstructural variation observed within different size powder particles and within individual ones.

1. Background

The control of microstructure during consolidation of rapidly solidified (RS) powders is an important practice for developing optimum properties and retaining the benefits of rapid solidification. Three Al–Cr alloys containing additions of Zr and Fe have been fabricated via cold compaction and hot extrusion. In the present work the consolidation behaviour in terms of the microstructural characteristics will be presented. Consequently, useful information can be gained, in order to understand the formation and building of the structure of a sound potential engineering material. Moreover the different levels of the alloying elements constitute a guideline to understand the effect these elements play on the microstructure development and consequently the resultant mechanical properties.

The extrusion process is a convenient route by which metal powder compacts are forced through a die orifice of a particular shape and size and consequently are converted into a 100% dense product. The extrusion process has been extensively studied for cast metals and powder compacts [1–3]. In the case of metal powders, extrusion combines both consolidation and hot working in a single operation. An ideal load–displacement curve is illustrated in Fig. 1. At the beginning of extrusion the approximately 75%–90% dense billet breaks, expands and fills the container; this is the stage in which the extrusion load increases non-linearly with displacement, see Fig. 1 stage a. During this stage any entrapped gas escapes through the interconnecting pores and is expelled past the ram until the billet attains the theoretical 100% density. Subsequently, the load increases linearly up to a maximum (stage b). The deformation zone has not been established yet, but extrusion has commenced at some intermediate location as indicated on the load–displacement curve (Fig. 1). The peak load increment

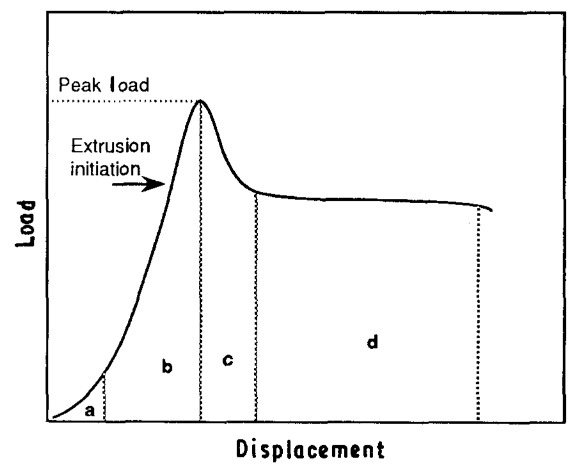

Figure 1 Typical load–displacement curve. (a) Compaction and set-up stage, (b) dislocation generation and multiplication, (c) decrease of the extrusion load and establishment of the shear zone, (d) steady state extrusion.

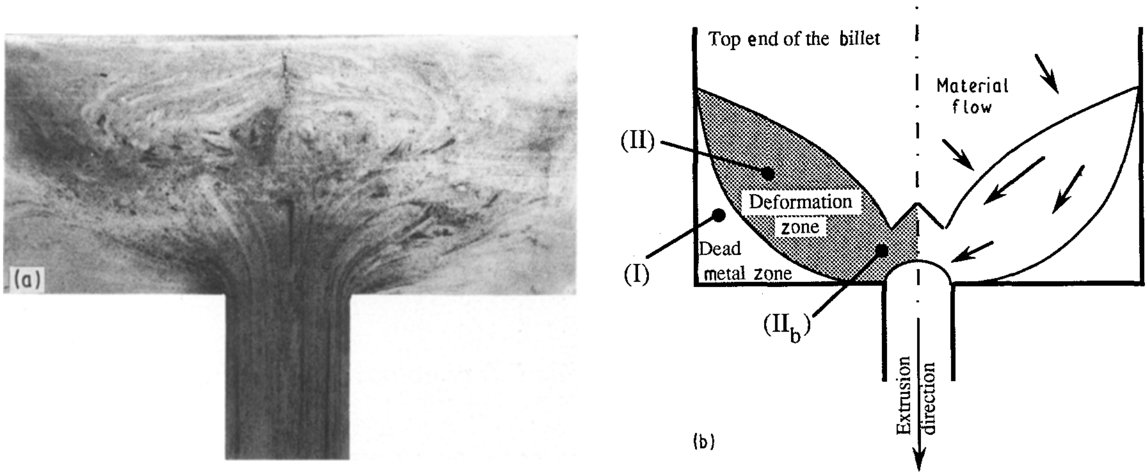

Figure 2 Flow characteristics of a partially extruded billet.

has been proved by Castle and Sheppard [4] to be associated with the excess energy required to establish a quasi-static deformation zone. During this stage, the billet is further compressed while dislocations play a dominant role in the creation of the deformation zone by their generation, migration and annihilation. After the peak load, the deformation zone is established while the load decreases to a minimum value, see Fig. 1, stage c. The minimum load remains constant throughout the remainder of the extrusion (Fig. 1, stage d), this stage is termed steady state. During steady state, the material passes through the quasi-static deformation zone in which consolidation occurs; the deformation zone remains constant and the rates of dislocation generation and annihilation are equal. The flow characteristics of a partially extruded billet during the steady state are illustrated in Fig. 2a, and Fig. 2b is a schematic representation of the material flow. Hence, it can be seen that the flow of the powder particles occurs from the periphery to the centre of the billet prior to extrusion through the die. The centre part of the billet moves forward more rapidly than the periphery. As the latter units enter the deformation zone the powder particles are first of all compressed and then pass diagonally with heavy shearing into the die. Hence, the central elements undergo minimum deformation mainly by compression of the powder particles corresponding to the extrusion ratio; whilst the layers near the surface undergo greater shear deformation and are stretched out along the periphery of the bar.

However, even though the extrusion characteristics are, in principle, similar for all three powder alloys, there are significant differences in powder microstructures. Therefore the microstructural characteristics of each alloy during processing will be presented separately. It should be recalled [5] that during processing the effect of the applied pressure significantly advances transformation kinetics and it is this unique combination of applied stress and elevated temperature which leads to structural changes during processing.

2. Experimental procedure

The powders were produced by inert gas atomization, and their chemical composition is given in Table I.

TABLE I Chemical composition of the three rapidly solidified alloys

Alloy	Cr (wt%)	Zr (wt%)	Fe (wt%)	Mn (wt%)
Al–5Cr–2Zr	5.15	2.01	0.09	< 0.02%
Al–6.43Cr–1.67Zr	6.43	1.67	0.19	< 0.02%
Al–4Cr–1Fe	3.99	—	0.99	< 0.02%

The average particle size has been reported [6] to be 24, 35 and 44 μm for the Al–5Cr–2Zr, Al–4Cr–1Fe and Al–6.43Cr–1.67Zr, respectively.

The fabrication of metal powders was performed in two distinct stages: cold compaction and hot extrusion. The billets were cold compacted approximately to a density of 87% and then rapidly (5–8 min) preheated to the desired temperature (450 °C), by using an induction furnace, and automatically transferred to the heated container of the extrusion press, which was maintained at 400 °C. The billets were then partially extruded into the steady state region. The partially extruded billets were removed from the press and water quenched within approximately 2 min.

To study the flow pattern during consolidation, a partially extruded billet sectioned in half, was polished and etched with a mixed acids solution ($HCl/HNO_3/HF$), see Fig. 2.

For microstructural assessment, thin discs were prepared from specimens extracted from various positions of the partially extruded billets, as indicated in Fig. 2. They were then thinned using a conventional electropolishing jet technique in a methanol solution of 1.5% HNO_3 and 5% $HClO_4$ at − 40 °C and 20 V. The study was performed by using a JEM-2000FX with an accompanying STEM attachment and Links energy dispersive X-ray analysis unit.

X-ray analysis was also conducted by using a Philips diffractometer with filtered CuK_α radiation on samples taken from various places from the partially extruded billets.

3. Results and discussion

3.1. Al–4Cr–1 Fe

Fig. 3 shows typical example of the microstructure of

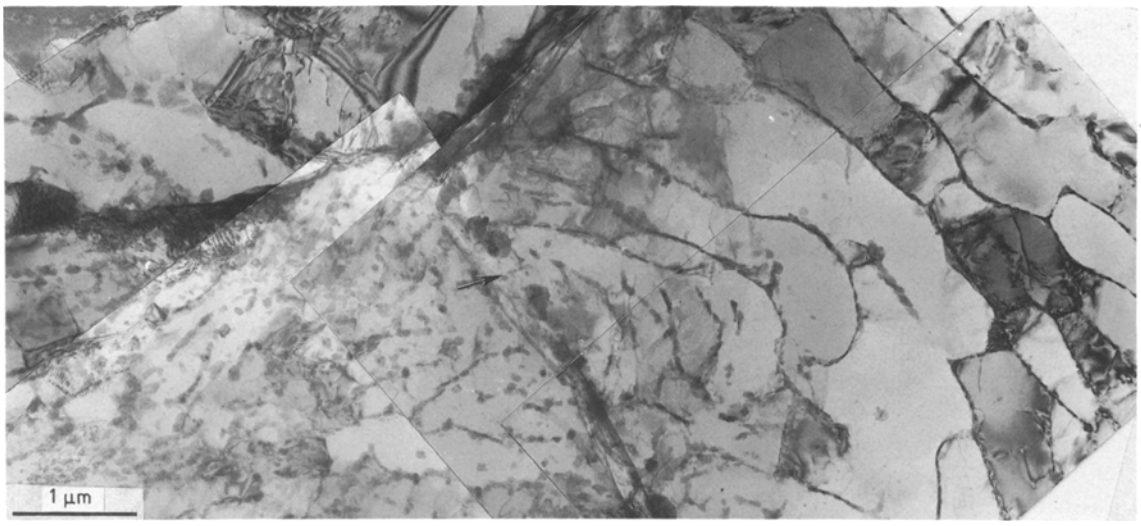

Figure 3 Typical microstructure of the dead metal zone for the Al–4Cr–1Fe alloy.

the dead metal zone (Fig. 2, location I). The structure of the compacted and hot-pressed powders in the partially extruded billet also demonstrates the development of a heterogeneous microstructure in the final extruded product [6]. The powder particles are closely packed together but have experienced minimal deformation. It can also be deduced that the powder particles exhibit a cellular morphology, which has also been reported previously [7], with similar microstructural features differentiated by their size, i.e. the cell size increases with increasing powder particle size. During induction heating, decomposition of the rapidly solidified microstructure commences at the intercellular network (also reported following a previous study of the decomposition behaviour of the atomized powders [8]) due to the high driving force for phase transformations in these solute-enriched areas. EDX analysis indicated that the precipitates formed are Fe-rich, but unfortunately, due to their very fine form, cannot be identified uniquely. The microstructure within the cells is devoid of second-phase particles indicating that during induction heating the time available was too short to allow precipitation to occur. The oxide layer surrounding the powder particles may be observed impeding metal/metal contact and thus interparticle bonding is poor. This is the reason that even though 100% density has been achieved the maximum strength is only obtained after the material passes through the deformation zone. In some instances the oxide film has been fragmented, as illustrated in the arrowed example in Fig. 3.

Consolidation occurs within the deformation zone. When the powder particles first enter the deformation zone, they have little resistance to shear and therefore the intermetallic bonds formed during compaction, Fig. 1, stage (a) fracture easily. Part of the deformation energy input during extrusion is utilized for the shearing of powder particles, thus building a coherent material. In the shear zone (Fig. 2, location II) the compacted powder particles and consequently the cells are elongated along the flow direction as illustrated in Fig. 4a. The original primary cell boundaries are now identifiable by precipitate stringers. These arrays

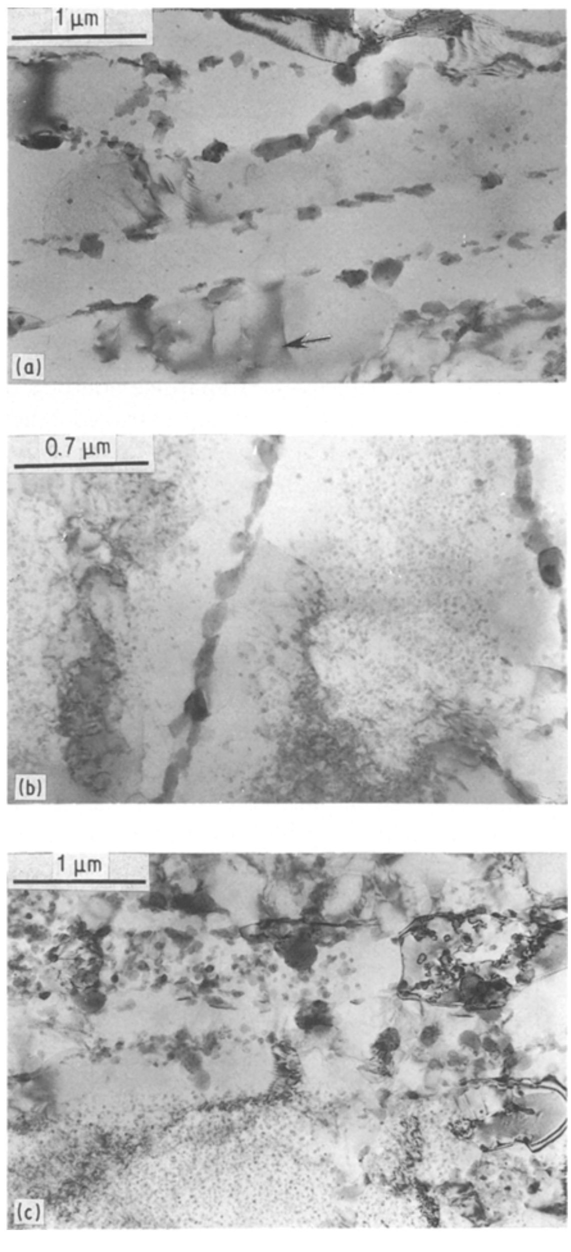

Figure 4 Microstructures of the intense shear zone for the Al–4Cr–1Fe alloy: (a) cells are aligned along the extrusion flow, (b) homogeneous precipitation within primary segregation-free areas, (c) structural heterogeneity.

are composed of discrete and uniquely identifiable Fe-rich precipitates [8] formed during decomposition of the intercellular network. As the material travels within the deformation zone, the precipitation reactions are enhanced by applied shear stress inherent in the extrusion process and the elevated temperature of the operation [9]. In primary segregation-free areas, such as in the centre of cells, or in small powder particles in which during rapid solidification a partitionless solidification front was developed [7], homogeneous nucleation and subsequent growth of second-phase particles occurs, see Fig. 4b. In this figure, a precipitate-free zone around a precipitate array is discernible, attributed to a solute-depleted zone surrounding the primary intercellular network. The structural heterogeneity, shown in Fig. 4c, observed within the deformation zone at location II_b in Fig. 2, is typical of powder metallurgy microstructures and is caused by the heterogeneity of the microstructure of the as-atomized powder particles. Different size liquid droplets solidify under different solidification mechanisms, thus resulting in structural heterogeneities [7]. The effect is exaggerated during thermomechanical working demonstrating the influence of strain-assisted diffusion on precipitation kinetics which commences at the solute-rich areas. Finally, during this stage, the oxide layer surrounding the powder particles fragments, forming submicrometre oxide particles finely dispersed within the as-extruded microstructure, which cannot be distinguished from the precipitates. Fragmentation of the oxide layer permits metal/metal contact and thus improves interparticle bonding. The heterogeneity within the partially extruded billet is expected to result in heterogeneity in the mechanical properties. Hardness is an acceptable measure of the resistance of the material to plastic deformation, and hence may be used to differentiate between structure; however, a proper assessment of the mechanical properties can only be achieved via tensile properties. Fig. 5 illustrates the variation of hardness within the partially extruded billet in which it can be seen that the hardness remains almost constant throughout the billet. This is perhaps a surprising observation but the reader should recall that during passage through the deformation zone the undercooled particles are subject to substructure formations, particle coarsening and precipitation reaction. It would appear that in this specific alloy these processes are acting such that hardening and softening processes are balanced, no doubt assisted by the temperature rise from rear to front of billet of about 30 °C [8].

It is interesting to compare the structure of the deformation zone with the microstructure of an *in situ* heated powder sample, at 450 °C for 25 min, see Fig. 6. During extrusion, due to the short time available for transformations, the microstructural features observed can be classified into two groups, coarse precipitates at the intercellular network and fine dense precipitation in the primary supersaturated areas where solute segregation is limited to a small area around the formed nuclei. In the undeformed specimen there is time available for solute segregation thus resulting in coarser precipitates evenly distributed with the cells. Finally, the as-extruded microstructure is heterogeneous, as-expected, composed of coarse and fine bands in intimate contact. A typical microstructure is shown in Fig. 7.

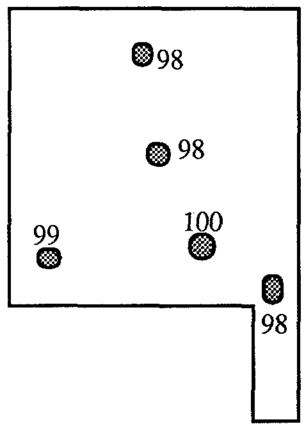

Figure 5 Hardness at different locations within the partially extruded billet for the Al–4Cr–1Fe alloy.

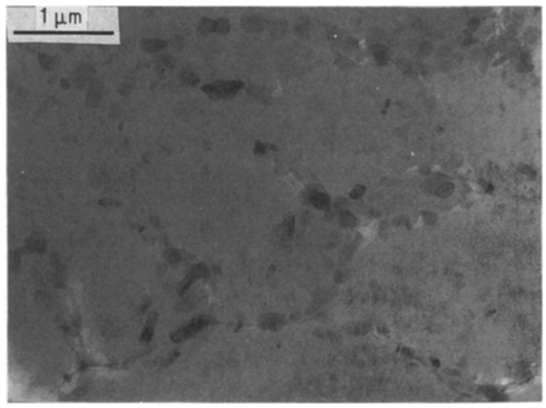

Figure 6 Typical microstructure of an *in situ* heated powder sample (450 °C, 25 min) for the Al–4Cr–1Fe alloy.

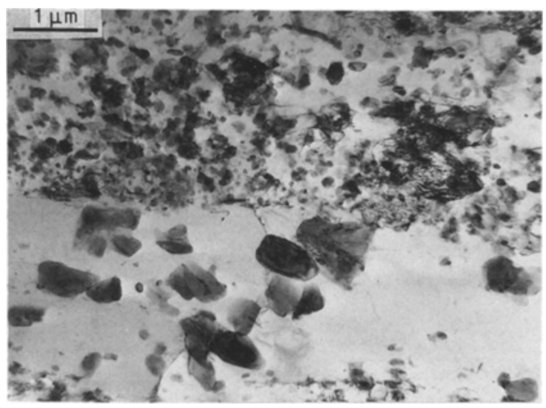

Figure 7 Heterogeneous as-extruded microstructure at 450 °C for the Al–4Cr–1Fe alloy.

3.3. Al–5Cr–2Zr

Fig. 8a–c illustrates typical microstructure of a specimen taken from the dead metal zone, Fig 2, location I. As-expected, powder particles in intimate contact can

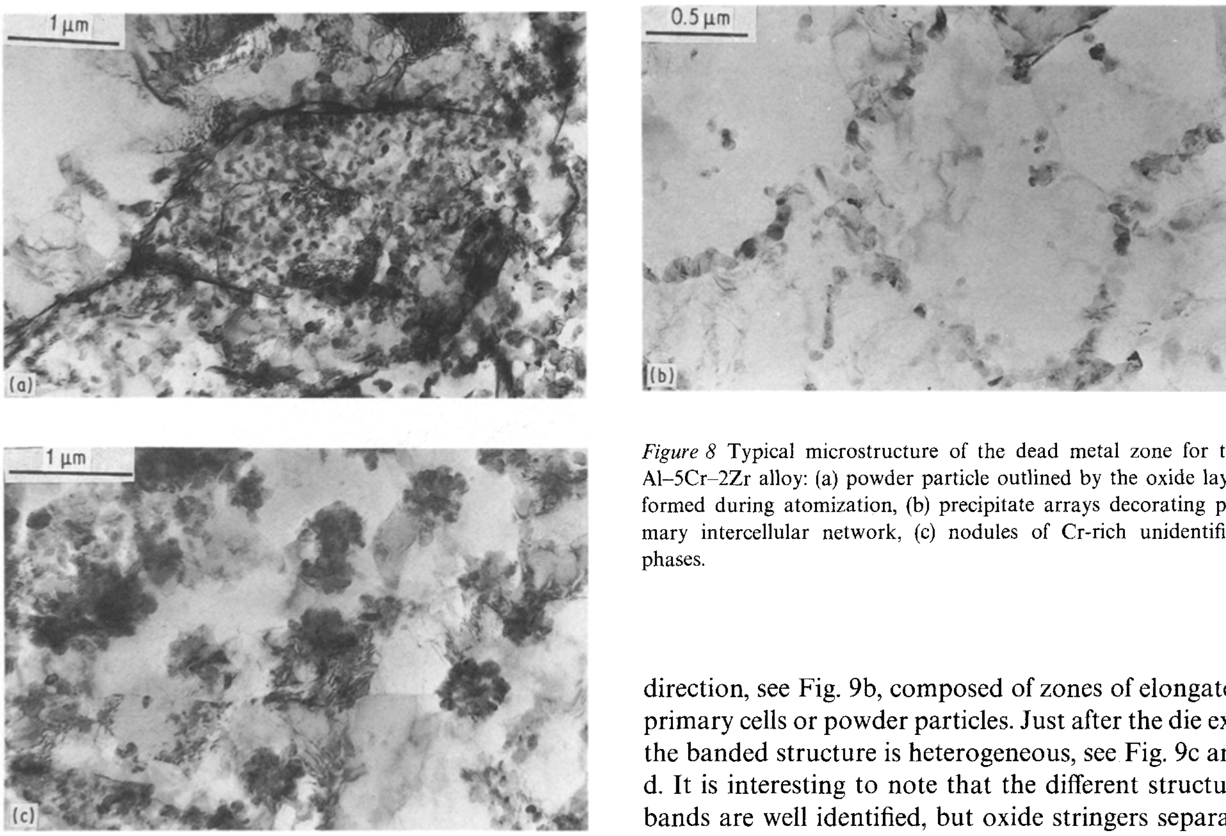

Figure 8 Typical microstructure of the dead metal zone for the Al–5Cr–2Zr alloy: (a) powder particle outlined by the oxide layer formed during atomization, (b) precipitate arrays decorating primary intercellular network, (c) nodules of Cr-rich unidentified phases.

be discerned, exhibiting different morphologies depending upon the original as-atomized powder microstructure. Fig. 8a illustrates a structure composed of uniformly distributed spherical precipitates, termed type D, whereas in Fig. 8b precipitates decorating primary cell boundaries can be seen. The latter morphology is typical of a cellular microstructure, where transformation of the powder microstructure has commenced at the solute-rich cell boundaries, which are now decorated with very fine $Al_{13}Cr_2$. The type D microstructure has also been observed in as-atomized powder particles [7] suggesting that during induction heating no appreciable phase transformation occurs to modify the microstructure. This is not the case in those particles which exhibit cellular morphologies and at the solute-rich intercellular network the driving force for transformation is very high. Coarse structures have also been observed, see Fig. 8c, composed of nodules of Cr-rich phases (EDX analysis indicated approximately 23 wt% Cr). The latter originate from powder particles in which high-temperature Cr-rich phases were formed in the melt. Subsequently, these Cr-rich phases act as nucleation sites for further precipitation eventually resulting in the precipitate clusters observed. Finally, it should be noted that X-ray diffraction analysis indicated reflections of metastable $ZrAl_3$ which probably precipitated during induction heating. A closer look at Fig. 8c shows the existence of ultra-fine precipitates within aluminium subgrains.

Similar to in the Al–4Cr–1Fe alloy, within the intense shear zone precipitation reactions are aided by the effect of shear, thus resulting in precipitation of very fine phases, see Fig. 9a (location II, Fig. 2). Near the die exit the structure is elongated along the flow direction, see Fig. 9b, composed of zones of elongated primary cells or powder particles. Just after the die exit the banded structure is heterogeneous, see Fig. 9c and d. It is interesting to note that the different structure bands are well identified, but oxide stringers separating them cannot be distinguished, suggesting that during extrusion the bonding of powder particles is completely efficient. The structure, marked "P", shown in Fig. 9d may well originate from segregation-free areas, observed in the as-atomized powders [7], where during high-temperature deformation, decomposition of the supersaturated solid solution areas has occurred, resulting in fine spherical and needle-shaped precipitates nucleated within the matrix.

Hardness measurements carried out at different positions of the partially extruded billet showed an unequivocal decrease in hardness (approximately 30%) proceeding from the top end of the billet towards the die exit, see Fig. 10. Clearly, during induction heating, precipitation of metastable $ZrAl_3$ has resulted in a harder matrix. On the other hand, the heat generated during deformation also aided by the dynamic recovery mechanisms resulted in a rapid softening.

3.4. Al–6.43Cr–1.67Zr

The dead metal zone may again be used as an illustration of the starting microstructure to be developed during mechanical working. Powder particles outlined by the oxide film formed during atomization can clearly be seen in Fig. 11a. Two different microstructural morphologies were observed which could be related directly to the size of intermetallic particles distributed within the matrix, see Fig. 11b and c. It can be observed that the second-phase particles are aggregates of individual precipitates. It has been well documented in another publication [7] that the aggregates, present in the dead metal zone, were formed during atomization by homogeneous nucleation in the liquid droplet prior to atomization. In the small powder particles the population of aggregates is higher,

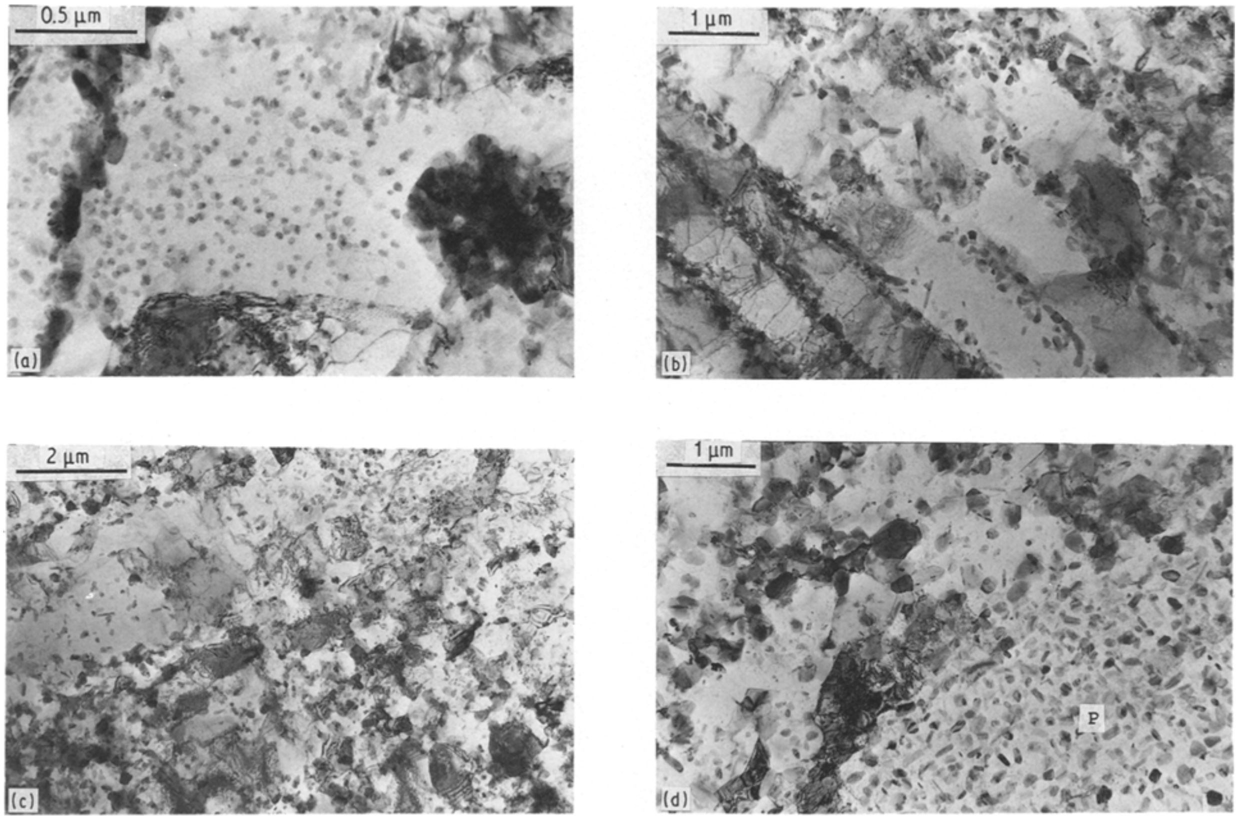

Figure 9 Microstructures of the intense shear zone for the Al–5Cr–2Zr alloy: (a) homogeneous precipitation due to shear assisted phase transformations, (b) elongated microstructure in the extrusion direction, (c, d) microstructural heterogeneity.

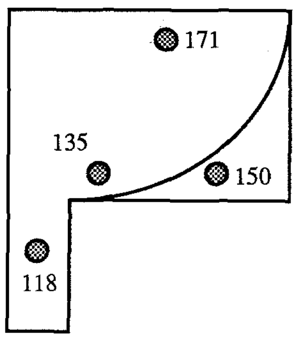

Figure 10 Variation of hardness within the partially extruded billet of the Al–5Cr–2Zr alloy.

whereas in the larger particles fewer and coarser aggregates are discernible having a flower-type morphology of petals stemming from a central core. The formation of the aggregates could be attributed to the solidification kinetics during atomization. In the larger droplets the time available for solute segregation allowed formation of coarser aggregates, resulting in a matrix with less solute content and thus a smaller population of intermetallics. The conclusion drawn so far is that during induction heating, except from fine precipitation of $ZrAl_3$, proved by X-ray diffraction analysis, other phase transformations do not occur and the microstructure remains more or less unaffected.

A typical example of the interparticle bonding occurring within the deformation zone is illustrated in Fig. 12a. Two particles exhibiting different morphologies are in intimate contact; the original oxide film has been fragmented and aligned in the direction of flow, as arrowed. Towards the die exit the structure is fibrous and heterogeneous, see Fig. 12b, but the powder particles have lost their identity indicating that consolidation has occurred. The coarser aggregates, which were observed in the as-atomized powder particles and were unaffected by induction heating, transform into a single Cr-rich phase, which cannot easily be identified (because it is very thick and a crystallographic study is not within the aim of the present work), again due to the combined effect of heating and deformation. A comparison between an aggregate having flower-type morphology and one in which growth of a single phase has started from the core of the flower and progressed further, is illustrated in Fig. 12c and d, termed "flower" and "cored" aggregates, respectively. EDX analysis carried out at different locations of the specimen indicated that firstly the chemical composition varied slightly between flower and cored aggregates, see Table II, and secondly the precipitate-free aluminium matrix subgrains contain very small amounts of Cr in solid solution, whereas most of the Zr is kept in solution, indicating that most of the Cr has precipitated in Cr-rich intermetallic particles.

Finally, similar to in the Al–5Cr–2Zr alloy, the hardness varies within different locations of the partially extruded billet, see Fig. 13. Precipitation of $ZrAl_3$ has occurred during induction heating; however, without leading to a dense precipitation, because it was shown by EDX analysis that most of the Zr is retained in the solid solution. The fine $ZrAl_3$

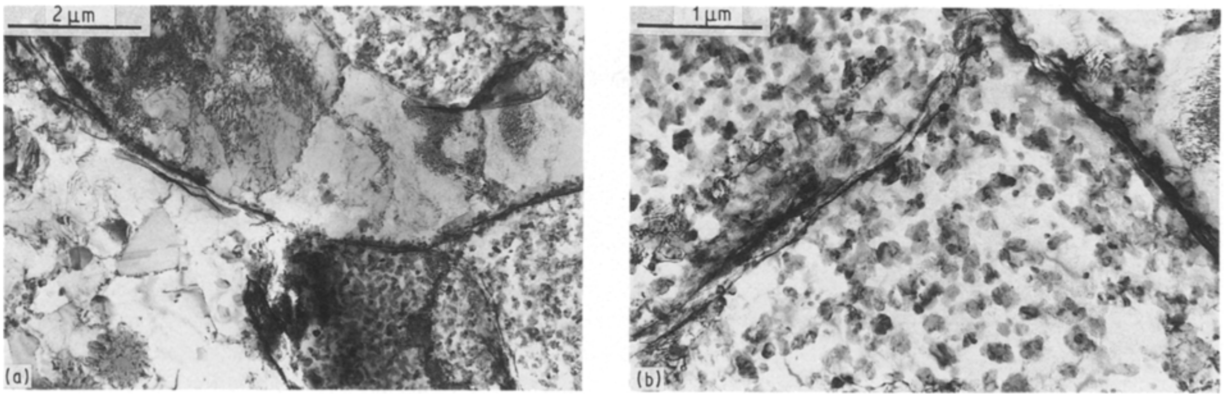

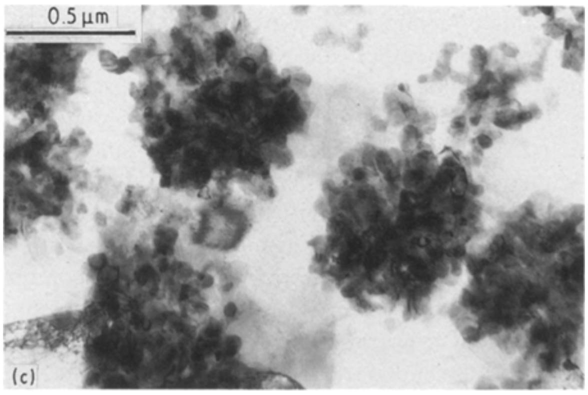

Figure 11 Typical microstructure of the dead metal zone for the Al–6.43Cr–1.67Zr alloy: (a) powder particle in intimate contact separated by the oxide film, (b, c) different size intermetallic particles evenly distributed within the matrix.

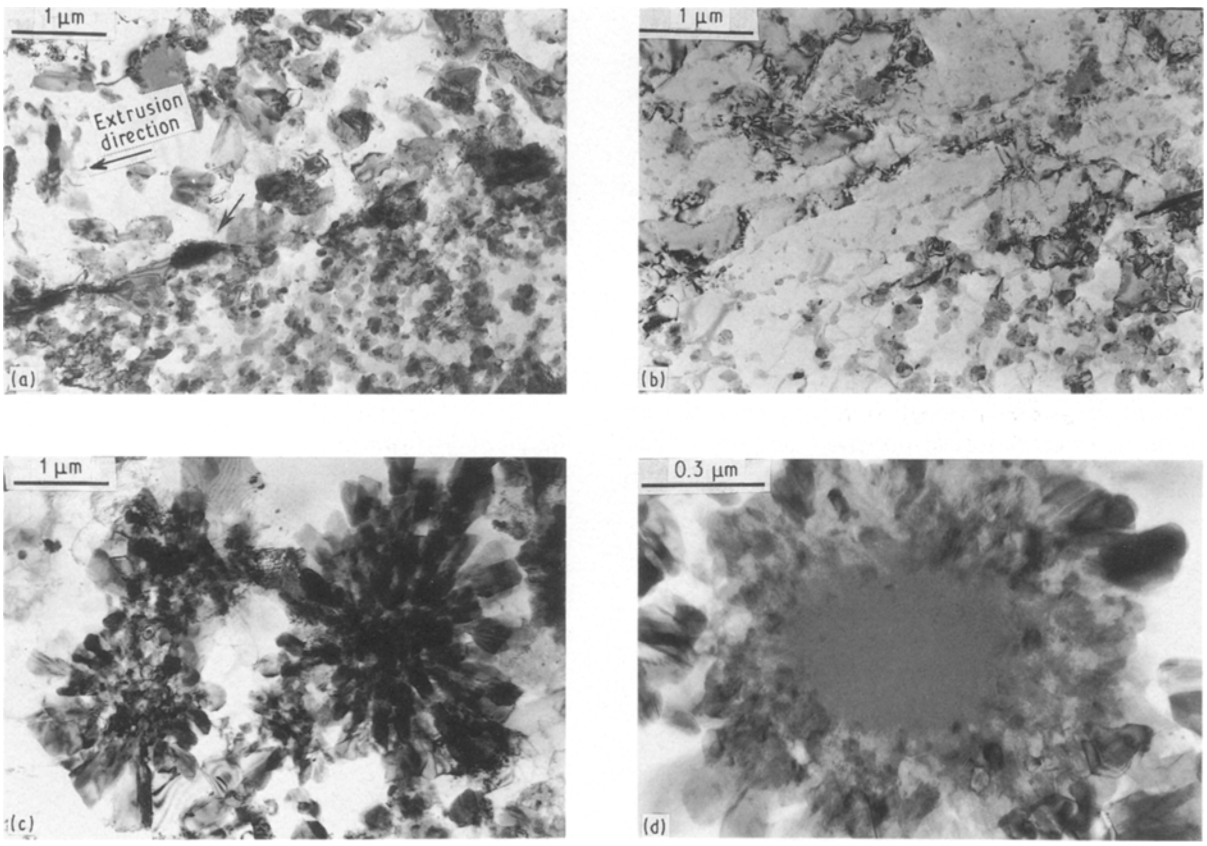

Figure 12 Typical microstructure of the deformation zone for the Al–6.43Cr–1.67Zr alloy: (a) fragmentation of the oxide film, (b) heterogeneous microstructure near the die exit, (c) "flower" type aggregate (untransformed), (d) "cored" aggregate (transformed).

TABLE II EDX analysis at different points of a specimen near the die exit from the Al–6.43Cr–1.67Zr alloy

	Al (wt%)	Cr (wt%)	Zr (wt%)	Si (wt%)
Aluminium subgrains	96.1 ± 0.2	1.3 ± 0.1	1.4 ± 0.1	1.2 ± 0.2
Untransformed aggregates	73.4 ± 0.6	24.5 ± 0.5	0.8 ± 0.1	1.3 ± 0.1
Transformed aggregates	71.7 ± 0.5	25.3 ± 0.6	1.0 ± 0.1	2.1 ± 0.3

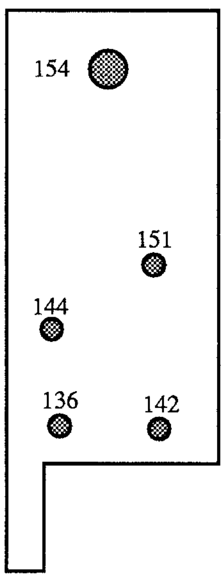

Figure 13 Variation of hardness within the partially extruded billet of the Al–6.43Cr–1.67Zr alloy.

precipitates strengthen the matrix as demonstrated at the back end of the billet, having hardness 154, whereas softening of the matrix has taken place during high-temperature deformation and has occurred within the deformation zone. The deformation mechanism was dynamic recovery leading to a substructure of subgrains of low misorientation, see Fig. 12b.

4. Conclusions

Consolidation of the loose powder particles and attainment of the full strength occurs during the extrusion thermomechanical process. The powder particles are outlined by the oxide film, formed during atomization, which breaks within the deformation zone due to heavy shearing, resulting in the interparticle bonding.

The transformation kinetics are aided by the shearing and the temperature rise during extrusion. In the Al–4Cr–1Fe and Al–5Cr–2Zr alloys, rapid solidification results in microstructures having mainly cellular morphologies in which, during subsequent thermomechanical processing, decomposition starts from the solute-rich intercellular network by the formation of small discrete precipitates. In the Al–6.43Cr–1.67Zr alloy, the coarse as-atomized structure, composed mainly of aggregates of individual precipitates, decomposes when the material passes through the deformation zone. Decomposition of the aggregates occurs in terms of a single phase growing from the centre of the aggregate rather than mechanical dispersion during extrusion.

The final as-extruded microstructure is heterogeneous, and is attributed to the inhomogeneity of the original powder particles being enhanced by the phase transformation occurring during processing. In order to produce a more homogeneous microstructure an alloy with less Cr and more Zr content is recommended. Chromium promotes the formation of coarse phases, and iron promotes the formation of eutectics at the intercellular network, thus both resulting in microstructural heterogeneity. On the other hand, zirconium is mainly in solid solution or in fine form possibly contributing to enhanced strength without promoting heterogeneity. A detailed investigation of the mechanical properties of the as-extruded material will reveal more useful information as far as alloy selection criteria is concerned.

References

1. H. McSHANE, PhD thesis, University of London (1978).
2. R. D. PARKINSON, PhD thesis, University of London (1983).
3. R. P. VIEROD, PhD thesis, University of London (1983).
4. A. F. CASTLE and T. SHEPPARD, *Metals Technol.* Oct. (1976) 465.
5. E. K. IOANNIDIS, G. MARSHALL and T. SHEPPARD, *J. Mater. Sci.* **23** (1988) 1486.
6. E. K. IOANNIDIS and T. SHEPPARD, *Mater. Sci. Technol.* **6** (August, 1990) 749.
7. *Idem, ibid.* **6** (June, 1990) 528.
8. *Idem, J. Mater. Sci.* **25** (1990) 3965.
9. E. K. IOANNIDIS, PhD thesis, University of London (1987).

Received 30 January
and accepted 19 November 1990